FOCUS ISSUE: CARDIAC RESYNCHRONIZATION THERAPY

MRI and Resynchronization

Propagation of Onset and Peak Time of Myocardial Shortening in Ischemic Versus Nonischemic Cardiomyopathy

Assessment by Magnetic Resonance Imaging Myocardial Tagging

Jaco J. M. Zwanenburg, MSc,* Marco J. W. Götte, MD, PhD,†‡ J. Tim Marcus, PhD,*
Joost P. A. Kuijer, PhD,* Paul Knaapen, MD,† Robert M. Heethaar, PhD,*
Albert C. van Rossum, MD, PhD†

Amsterdam and Groningen, the Netherlands

OBJECTIVES	We aimed to study the relation between onset and peak time of circumferential shortening and the direction of propagation of these parameters in both ischemic and nonischemic patients.
BACKGROUND	Peak time is often used to select patients for cardiac resynchronization therapy, whereas pacing influences only the onset times directly. Furthermore, it is unclear whether there is a consistent direction of propagation delay and whether this depends on the etiology.
METHODS	Magnetic resonance imaging myocardial tagging with high temporal resolution (14 ms) was applied to 29 patients (18 nonischemic, 11 ischemic) and 17 healthy control subjects. Time to onset (T_{onset}), to first peak ($T_{\text{peak,first}}$), and to maximum peak ($T_{\text{peak,max}}$) of circumferential shortening were determined. Three-dimensional vectors were calculated to denote the main direction of asynchrony.
RESULTS	In both patient groups, T_{onset} showed a significant positive relation with both $T_{\text{peak,first}}$ and $T_{\text{peak,max}}$; however, $T_{\text{peak,first}}$ correlated considerably better with T_{onset} than did $T_{\text{peak,max}}$ ($p < 0.0001$ for nonischemic, and $p < 0.01$ for ischemic patients). Moreover, the relations between T_{peak} and T_{onset} were stronger in the nonischemic patients than in the ischemic patients ($p < 0.001$). In nonischemic patients, the propagation of T_{onset} was consistently from septum to lateral wall. In the ischemic patients, however, no consistent direction of propagation was found. For both groups, the longitudinal propagation delays (between apex and base) were negligible compared with the short-axis delays.
CONCLUSIONS	The relation between peak time and onset time of shortening is strongest in nonischemic patients and is most consistent when time to first peak is used (instead of time to maximum peak). (J Am Coll Cardiol 2005;46:2215–22) © 2005 by the American College of Cardiology Foundation

Mechanical asynchrony seems to be a more appropriate parameter than electrical asynchrony for adequate selection of patients that are likely to respond to cardiac resynchronization therapy (CRT) (1,2). Because onset times of regional mechanical function are more directly influenced by pacing than peak times (3,4), onset times would be a logical measure for mechanical asynchrony. Nevertheless, onset times are relatively difficult to measure, whereby most asynchrony measures focus on peak times, using either displacement (5), velocity (6), or longitudinal strain and strain-rate (7,8). Although these studies have shown that asynchrony in peak times correlates well with the response to CRT, a direct comparison between peak time and onset time, justifying the use of peak times, is not available.

Furthermore, the direction of the asynchrony is often neglected by using the standard deviation over all available segments (9), the maximum asynchrony between any two measured locations (10), or by studying one fixed direction, normally the septum-to-lateral wall direction (5). Recently, however, Bader et al. (3) and Ghio et al. (4) reported interesting data from regional onset times of systolic velocity in patients with heart failure. Both studies reported that the lateral wall is the latest region in only one-third of the patients, suggesting a large spread in the direction of the asynchrony in these patients. From these data, the question arises as to the extent to which asynchrony is present between septum and lateral wall or whether other locations, including apex versus base, should be considered.

Intramural myocardial circumferential shortening, which can be measured by means of magnetic resonance imaging (MRI) tagging, is a strong parameter to study regional

Abbreviations and Acronyms

CRT	= cardiac resynchronization therapy
ECG	= electrocardiogram
EF	= ejection fraction
LV	= left ventricle/ventricular
MRI	= magnetic resonance imaging
OS	= onset of shortening
PS	= peak shortening
SV	= stroke volume
T_{onset}	= time to onset
$T_{peak,first}$	= time to first peak
$T_{peak,max}$	= time to maximum peak

mechanical function (11). The MRI tagging has already been applied successfully in dogs to study the regional timing of circumferential shortening in the left ventricle (LV) (12). Owing to recent developments, the temporal resolution of MRI tagging has become sufficient (14 ms) to study the regional timing of circumferential shortening also in human subjects (13).

In this study, MRI tagging was applied in both ischemic and nonischemic patients who were screened for CRT. The timing of circumferential shortening was analyzed for the following two research purposes: 1) to gain more knowledge of the relation between peak time and onset time of circumferential shortening, and 2) to study the three-dimensional propagation of the peak time and onset time over the LV. The propagation was characterized by a three-dimensional vector. This allowed a straightforward comparison between the longitudinal component of the propagation (apex vs. base) and the short-axis component. In the analysis, ischemic patients were distinguished from nonischemic patients to investigate whether differences were observed that could help to understand the lower response of ischemic patients to CRT compared with nonischemic patients (14,15).

METHODS

Subjects. Twenty-nine patients were selected from patients referred to our hospital to be screened for biventricular pacing. Inclusion criteria were: depressed LV function (ejection fraction [EF] ≤45% with MRI), wide QRS (≥120 ms), and New York Heart Association functional class II to IV. Eleven patients (age 66 ± 9 years, 4 women) were classified as ischemic (based on a history of myocardial infarction and/or significant coronary artery disease assessed by coronary angiography), and 18 (age 57 ± 14 years, 6 women) were nonischemic. All patients were in sinus
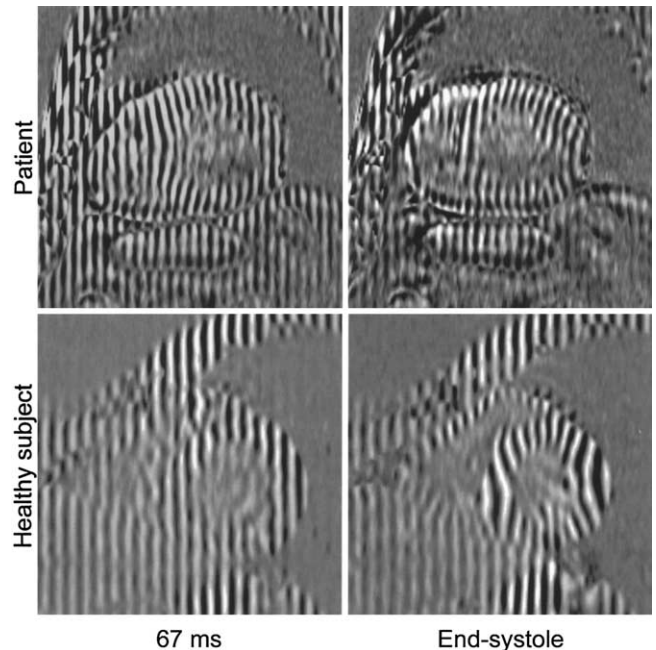
Figure 1. Example tagging images for a patient **(top)** and a healthy subject **(bottom)**. Early shortening occurs in the septum of the patient **(left)**, whereas this shortening is not preserved at aortic valve closure (end-systole, **right**).

rhythm, clinically stable, and received standard heart failure therapy, including diuretics, beta-blockers, angiotensin-converting enzyme inhibitors, and/or angiotensin II receptor blockers. Written informed consent was obtained according to our institutional guidelines. A group of 17 healthy subjects of whom the timing of shortening has been reported previously (13) served as control group.

Imaging. Complementary tagged (CSPAMM) myocardial images were acquired with a high temporal resolution of 14 ms, using steady state free precession imaging and a multiple brief expiration breath-hold scheme (13). Imaging parameters are given in Table 1, and example images in Figure 1. Images for two-dimensional strain analysis were acquired in five short-axis planes, evenly distributed over the LV. Steady state free precession cine imaging (without tagging) was performed with full coverage of the LV to assess LV volumes and EF.

Post-processing. STRAIN ANALYSIS AND GLOBAL FUNCTION. Circumferential strain ($epsilon_c$) curves were calculated for six circumferential segments, as previously described (13). End-diastolic volume, end-systolic volume, stroke volume (SV), and EF were derived from the cine images with the MASS software (version 5.1b; MEDIS, Leiden, the Netherlands).

Table 1. Magnetic Resonance Parameters of the Acquisitions

Acquisition	Voxel Size (mm³)	Matrix	Temporal Resolution (ms)	α	TR/TE (ms)	BW (Hz/pixel)
Tagging cines	1.2 × 3.8 × 6.0	256 × 78	14	20°	4.7/2.3	369
Conventional cines	1.3 × 1.3 × 6.0–8.0	256 × 208	35–48	60°	3.2/1.6	930

BW = receiver bandwidth; Matrix = number of readout × phase encoding samples; α = excitation flip angle; TE = echo time; TR = repetition time.

TIME TO ONSET OF SHORTENING. Time to onset of shortening (T_{onset}; in ms from the electrocardiogram [ECG] R-wave) was defined as the beginning of the down-slope of the circumferential strain curve and was semi-automatically determined as described in the Appendix of reference (13). To optimize the algorithm for patient data, the earliest allowed onset time (T_1) was set to 15 ms after the ECG R-wave. Furthermore, the onset time of shortening was regarded as missing when the goodness of fit was <0.85 or when regions were akinetic, which were defined as regions with a peak shortening of <3%. In case the algorithm could not determine T_{onset}, two observers (T. M. and J. J. M. Z.) reviewed the strain curve and determined in mutual agreement the T_{onset} for that curve. The observers regarded T_{onset} as missing if artifacts or akinesia made a determination of T_{onset} not possible.

The propagation of the onset of shortening was characterized by a three-dimensional vector, called the onset of shortening delay vector (OS-delay vector) (16). The first component of the OS-delay vector yields the delay between the septum and the lateral wall (positive: lateral wall later than septum); the second component is the delay between inferior (IN) and anterior (AN) (positive: AN later than IN); and the third component is the delay between apex and base (positive: base later than apex). Thus, this vector points from the earliest activated region to the latest, and its magnitude is a measure for the delay between these two regions. The vector was not calculated when T_{onset} data were missing in 50% or more of the myocardial segments.

TIME TO PEAK SHORTENING. In healthy subjects, time to peak shortening (T_{peak}) was defined as the time of maximum shortening (13). Multiple shortening waves might exist in patients (Fig. 2). Therefore, two peak time parameters were determined: the time to the first peak of shortening ($T_{peak,first}$) and the time to the maximum peak of shortening ($T_{peak,max}$). The first peak was detected automatically with the first zero-crossing in the strain-rate from a negative strain rate (circumferential shortening) to a positive

strain rate (circumferential lengthening). The peak shortening delay vector (PS-delay vector) was defined in complete analogy to OS-delay vector. The peak times were also reviewed and adjusted or rejected by two observers (T. M. and J. J. M. Z.) in mutual agreement.

Statistical analysis. Multilevel regression was used to investigate whether the onset time was associated with the peak time (MLwiN, version 1.02.0002; Centre for Multilevel Modelling, London, United Kingdom) (17). Multilevel regression allows for the calculation of regression coefficients corrected for the dependency that might exist in the observations owing to the hierarchy of the data (segments are clustered within slices, and slices are clustered within subjects). Standardized regression coefficients were calculated, which can be regarded as partial correlation coefficients. These standardized regression coefficients were used to compare the difference in performance of the two peak time parameters ($T_{peak,first}$ and $T_{peak,max}$) and to compare the difference between the relations found for the two patient groups (ischemic and nonischemic).

Because the multilevel analysis revealed that the dependency was only relevant on the subject level (i.e., the relation between T_{onset} and T_{peak} differs significantly between subjects, but not between slices), individual Pearson correlation coefficients between T_{onset} and T_{peak} are also presented. The individual correlation coefficients were calculated with the data from the available segments of each heart: five slices × six segments minus possible missing values (pair-wise).

To explore the direction of propagation of T_{onset} and T_{peak}, the components of the OS-delay vectors and the PS-delay vectors were compared between patients and control subjects with unpaired t tests assuming unequal variances. Values are presented as means ± SD, and p values <0.05 were regarded as significant.

RESULTS

Example strain curves for two segments of the heart are shown in Figure 2. Note the difference in $T_{peak,first}$ and
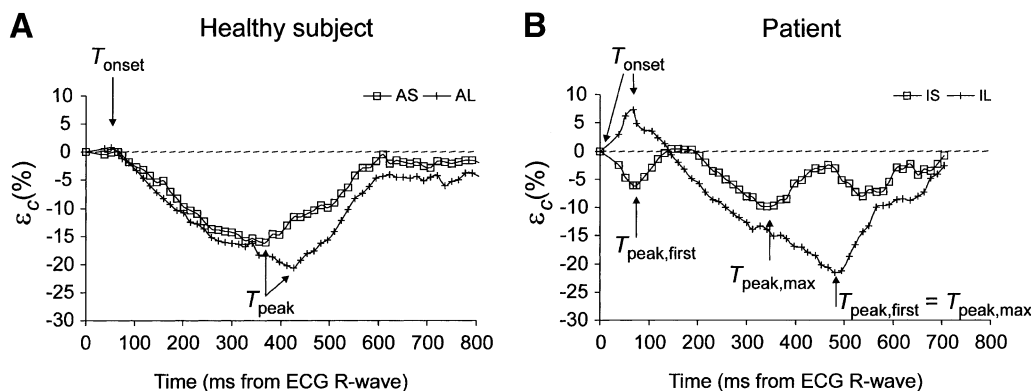
Figure 2. Example circumferential strain curves over time for one septal segment and one lateral segment of a mid ventricular slice, showing the definitions of the several timing parameters. **(A)** Healthy subject, showing synchronous shortening. **(B)** Nonischemic patient with multiple shortening waves in the septum, leading to a first peak and a maximum peak of shortening. AL = anterolateral; AS = anteroseptal; ECG = electrocardiogram; IL = inferolateral; IS = inferoseptal; T_{onset} = onset time of shortening; $T_{peak,first}$ = time to first peak of shortening; $T_{peak,max}$ = time to maximum peak of shortening.
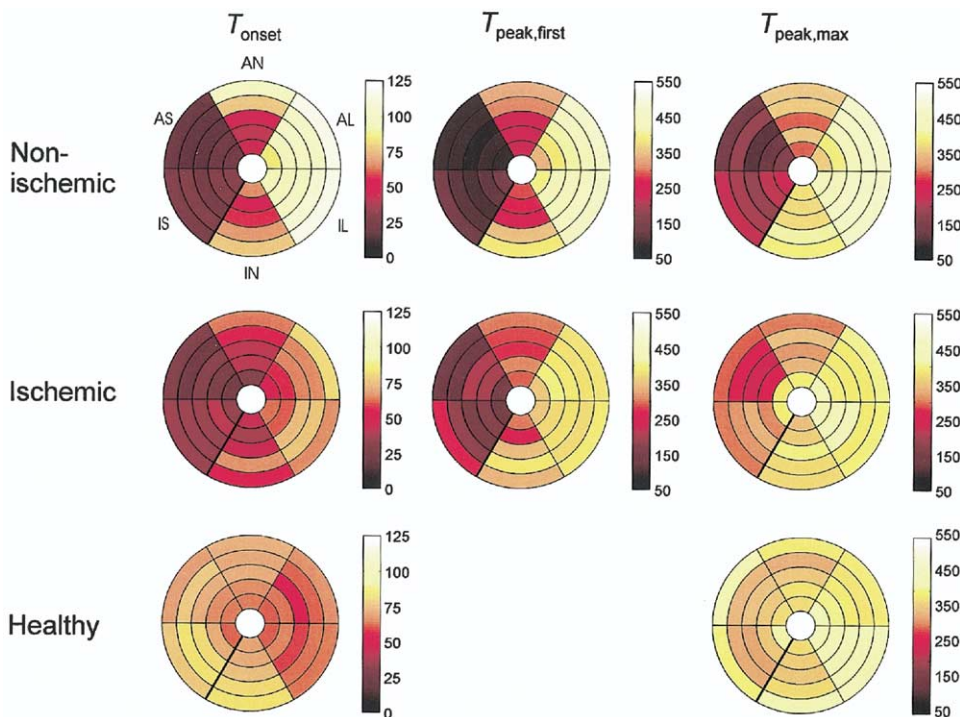
Figure 3. Mean maps of the timing of shortening, illustrating the different timing patterns in nonischemic patients, ischemic patients, and healthy subjects. Note the similarity in the patterns between onset time and peak time for the nonischemic patients. These patterns are less similar and less distinct for the ischemic patients. The segments are defined in the **bulls-eye top left**. T_{onset}, $T_{peak,first}$, and $T_{peak,max}$ all in ms from the ECG R-wave. AN = anterior; IN = inferior; other abbreviations as in Figure 2.

$T_{peak,max}$ in the septal segment of the patient. Figure 3 illustrates the timing of shortening for the two patient groups and the healthy volunteers. The uncoordinated onset of shortening in the patients is clearly visible from both earlier and later onsets times compared with the healthy subjects. No significant difference in global function was observed between the ischemic and the nonischemic group (Table 2).

Relation onset time versus peak time. A significant positive relation was found between onset time and peak time for both $T_{peak,first}$ and $T_{peak,max}$ and for both nonischemic and ischemic patients (Table 3); however, $T_{peak,first}$ correlated better with T_{onset} than $T_{peak,max}$ (p < 0.0001 in the nonischemic group, and p < 0.01 in the ischemic group). Moreover, the relations were considerably stronger for the nonischemic patients than for the ischemic (p < 0.001). In the normal control subjects, a slight but significant negative relation between T_{onset} and T_{peak} was observed, as described earlier (13).

Table 2. Global Function Parameters of the Subjects

Global Function Parameter	Healthy Subjects (n = 17)	Nonischemic (n = 18)	Ischemic (n = 11)
End-diastolic volume (ml)	171 ± 31	325 ± 110	292 ± 90
End-systolic volume (ml)	76 ± 20	261 ± 117	237 ± 95
Stroke volume (ml)	96 ± 22	64 ± 23	54 ± 14
Ejection fraction (%)	56 ± 5	23 ± 12	21 ± 11
Heart rate (beats/min)	59 ± 8	70 ± 12	67 ± 9

Values are means ± SD.

The individual correlation coefficients are visualized in Figure 4a. In the nonischemic patients, 16 of the 18 subjects showed a significant correlation between T_{onset} and $T_{peak,first}$ (Fig. 4A), and 14 of the 18 subjects had a significant correlation between T_{onset} and $T_{peak,max}$ (Fig. 4B). Note also the better performance of $T_{peak,first}$ compared with $T_{peak,max}$ regarding the correlation with T_{onset}, illustrating the findings of the multilevel analysis.

In the individual ischemic patients, only 7 of the 11 subjects showed a significant correlation between T_{onset} and $T_{peak,first}$ (Fig. 4C),, and only 6 of the 11 showed a significant correlation between T_{onset} and $T_{peak,max}$ (Fig. 4D).

The spatial distribution in T_{onset}, $T_{peak,first}$, and $T_{peak,max}$ is shown for two nonischemic patients in Figure 5. The first patient (Fig. 5, upper row) had a good correlation for both T_{onset} versus $T_{peak,first}$ and for T_{onset} versus $T_{peak,max}$, whereas the second patient had only a good correlation between T_{onset} versus $T_{peak,first}$ but not between T_{onset} versus $T_{peak,max}$.

Propagation of onset time and peak time. The OS-delay vector could be calculated in all nonischemic patients, in 8 of the 11 ischemic patients, and in all healthy subjects. The PS-delay vector based on $T_{peak,first}$ could be calculated in 17 of the 18 nonischemic patients and in 10 of the 11 ischemic patients. The PS-delay vector based on $T_{peak,max}$ could be calculated in all patients and in all healthy subjects.

In the nonischemic patient group, the asynchrony of T_{onset} in the short-axis direction dominated the asynchrony in the long-axis direction, because the magnitude of the

Table 3. Results From the Multilevel Regression Analysis of the Relation Between Onset Time (Outcome Variable) and Peak Time of Shortening (Independent Variable)

| Relation	Constant (ms)	Regression Coefficient	rho
T_{onset} vs. $T_{peak,first}$ for			
Nonischemic patients	3 ± 2	$0.23 \pm 0.01^*$	$0.85 \pm 0.04\dagger\ddagger$
Ischemic patients	7 ± 5	$0.15 \pm 0.01^*$	$0.62 \pm 0.06\S$
T_{onset} vs. $T_{peak,max}$ for			
Nonischemic patients	$8 \pm 4\|$	$0.18 \pm 0.01^*$	$0.66 \pm 0.05\P$
Ischemic patients	$18 \pm 8\|$	$0.09 \pm 0.02^*$	0.37 ± 0.08
Normals	$91 \pm 6^*$	$-0.06 \pm 0.01^*$	-0.18 ± 0.04

$^*p < 0.0001$ vs. null-hypothesis; $\dagger p < 0.0001$ vs. corresponding relation in ischemic patients, $\ddagger p < 0.0001$ vs. relation using $T_{peak,max}$ instead of $T_{peak,first}$, $\S p < 0.01$ vs. relation using $T_{peak,max}$ instead of $T_{peak,first}$, $\| p < 0.05$ vs. null-hypothesis, $\P p < 0.001$ vs. corresponding relation in ischemic patients. The standardized regression coefficient rho (which can be interpreted as partial correlation coefficient corrected for the dependency in the data) is used to compare the difference in performance between the two peak time parameters and to compare the difference between the two patient groups.

rho = standardized regression coefficient; T_{onset} = time to onset of shortening; $T_{peak,first}$ = time to first peak of shortening; $T_{peak,max}$ = time to maximum peak of shortening.

short-axis component of the OS-delay vector was a factor of 8 ± 9 (range: 0.3 to 38) larger than the long-axis component. Within the short-axis direction, the septum to lateral wall component was much larger than the AN-IN component (88 ± 30 ms vs. -6 ± 25 ms) (Table 4). The septum to lateral wall component was always positive (range: 5.1 to 115 ms), indicating that the septum was always earlier than the lateral wall in the nonischemic group. Compared with control subjects, the septum to lateral wall component pointed in the opposite direction and was much larger (88 ± 30 ms vs. -12 ± 10 ms, $p < 0.0001$) (Table 4). The

longitudinal component pointed from the apex to the base, although propagation was slightly delayed in comparison with the control subjects (22 ± 18 ms vs. 9 ± 7 ms, $p < 0.01$) (Table 4).

In the ischemic patient group, the short-axis component of the OS-delay vector was also much larger than in the long-axis component: a factor of 13 ± 18 (range 2.1 to 45.0); however, no consistent direction was observed within the short-axis component. The septum to lateral wall component ranged from -20 to 84 ms, indicating that the lateral wall was not always later than the septum. Also the
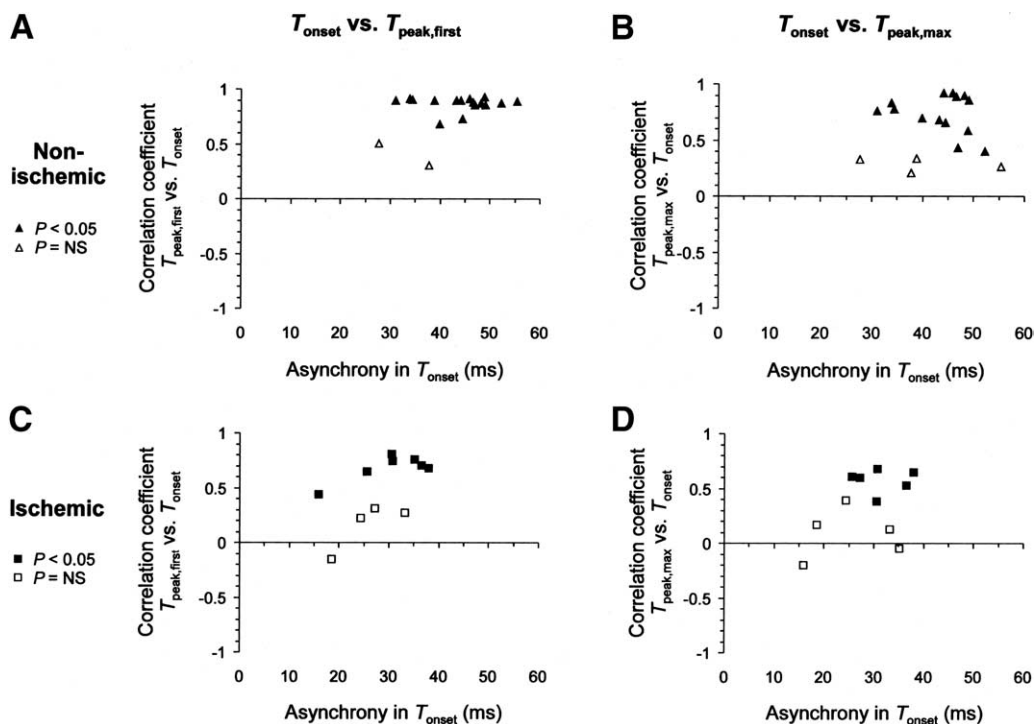
Figure 4. Individual correlation coefficients between onset time and peak time, plotted versus the individual asynchrony in T_{onset}. The asynchrony in T_{onset} is defined as the intra-subject variance in T_{onset} and is a measure for the range of values that is available for the correlation. Each data point represents one subject. **(Top row)** Correlation coefficients from nonischemic patients (n = 18), using **(A)** $T_{peak,first}$ and **(B)** $T_{peak,max}$. For some nonischemic patients, no association between $T_{peak,max}$ and T_{onset} exists, even when there is a large asynchrony in T_{onset}, indicating an important discrepancy between $T_{peak,max}$ and T_{onset}, which is not observed between $T_{peak,first}$ and T_{onset}. **(Bottom row)** Correlation coefficients from ischemic patients (n = 11) for **(C)** $T_{peak,first}$ and **(D)** $T_{peak,max}$. A considerable number of ischemic patients show a poor correlation between peak time and onset time, regardless of whether $T_{peak,first}$ or $T_{peak,max}$ is used. Abbreviations as in Figure 2.
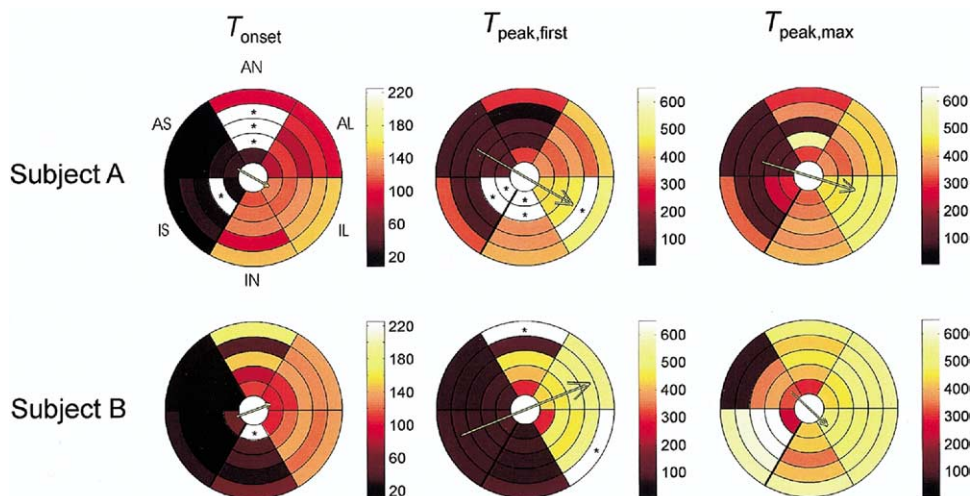
Figure 5. Individual maps of the timing of shortening, illustrating the difference in performance between $T_{peak,first}$ and $T_{peak,max}$. **(Subject A)** nonischemic patient for whom both $T_{peak,first}$ and the $T_{peak,max}$ correlated well with T_{onset}. **(Subject B)** nonischemic patient for whom only $T_{peak,first}$ correlated well with T_{onset}. *Missing values. Abbreviations as in Figures 2 and 3.

(relatively) larger SDs for the short-axis components of the OS-delay vector (Table 4) indicate that no consistent propagation pattern was found in the ischemic patient group.

In all patients, the PS-delay vector based on $T_{peak,first}$ showed generally a similar pattern of propagation as the OS-delay vector (Table 4). On average, the direction of the PS-delay vector based on $T_{peak,max}$ was also similar to that of the OS-delay vector, but in individual cases, important discrepancies were observed (Fig. 5).

An interesting observation was that the asynchrony, quantified as the magnitudes of the delay vectors, tended to be larger for the nonischemic patient group than for the ischemic patient group, although the global function characteristics (SV, EF, and heart rate) were similar (p > 0.11 for SV, and p > 0.5 for EF and heart rate). The observed differences were: 97 ± 22 ms versus 73 ± 27 ms for the

magnitude of the OS-delay vector (nonischemic vs. ischemic, p = 0.05); 371 ± 92 ms versus 264 ± 149 for the magnitude for the PS-delay vector based on $T_{peak,first}$ (p = 0.061); and 328 ± 111 ms versus 219 ± 78 ms for the magnitude of the PS-delay vector based on $T_{peak,max}$ (p < 0.005).

DISCUSSION

This study focused on two basal questions related to CRT. First, we studied whether peak time of regional myocardial shortening, which is normally used to assess LV asynchrony, is correlated to the onset time, which is most directly influenced by pacing. Second, we studied whether there is a consistent pattern in the propagation of onset and peak time. Both ischemic and nonischemic patients were studied with MRI myocardial tagging with high temporal resolution.

Table 4. Orthogonal Components of the Onset of Shortening Delay Vectors and Peak Shortening Delay Vectors for Both Patients and Normal Control Subjects

	Component of the Delay Vector (ms)		
Vector	**Septum → Lateral Wall**	**IN → AN**	**Apex → Base**
OS-delay vector for:			
Nonischemic patients	88 ± 30*	−6 ± 25	22 ± 18†
Ischemic patients	43 ± 39†	−0.1 ± 52	19 ± 12‡
Normals	−12 ± 10	−9 ± 9	9 ± 7
PS-delay vector based on $T_{peak,first}$ for:			
Nonischemic patients	351 ± 92	−45 ± 90	59 ± 37
Ischemic patients	233 ± 153	−4 ± 119	14 ± 42
PS-delay vector based on $T_{peak,max}$ for:			
Nonischemic	299 ± 124*	−57 ± 85	46 ± 60‡
Ischemic	127 ± 122	−65 ± 124	−14 ± 78
Normals	54 ± 19	−17 ± 26	2 ± 45

Values are means ± SD. A negative value means that the propagation is opposite to the direction indicated at the top of the column. *p < 0.0001, †p < 0.01, ‡p < 0.05 versus control subjects.
AN = anterior; IN = inferior; OS = onset of shortening; PS = peak shortening.

Onset time versus peak time. $T_{\text{peak,first}}$ yielded better correlations with T_{onset} than $T_{\text{peak,max}}$. This can be explained by the occurrence of multiple shortening waves in the early-activated regions (Fig. 2A). The actual peak value of each shortening wave is determined by regional wall stress and contractile force and might vary from region to region. As a consequence, whether maximum shortening occurs at the first, second, or third shortening wave is variable from region to region, leading to inconsistent $T_{\text{peak,max}}$ values.

The origin of the multiple septal shortening waves might be related to interaction of the left and right ventricles in combination with the weak contraction of the early activated septum (18,19). The effect of the interaction depends on several factors, including the compliance of the wall (influenced by fibrosis), wall stress, and contractility and might, therefore, vary from patient to patient.

From the regression coefficients between T_{onset} and $T_{\text{peak,first}}$ (Table 3) it can be observed that the asynchrony in $T_{\text{peak,first}}$ is an amplified version of the asynchrony in T_{onset}: the range in T_{onset} is 0.23 times the range in $T_{\text{peak,first}}$ (for the nonischemic patients), implying that the asynchrony in $T_{\text{peak,first}}$ is about 4 times larger than that in T_{onset}. This amplification might make $T_{\text{peak,first}}$ a more sensitive parameter to detect asynchrony than T_{onset}. The amplification in asynchrony might be related to the fact that early activated regions, which operate at a low load, have a short and weak contraction (18,20).

Propagation. Regardless of the etiology, the propagation delays occurred dominantly in the short-axis direction. In patients, the propagation of T_{onset} in the long-axis direction was only slightly delayed in comparison with the control subjects and directed from apex to base, which is the favorable direction, because it propels the blood towards the outflow tract.

For the nonischemic patients, the short-axis component of the propagation was very consistently directed from the septum to the lateral wall. For the ischemic patients, however, no consistent direction of the short-axis component of the propagation was found. Therefore, regarding the nonischemic patients, it is justifiable to focus only on the septum to lateral wall delay; but in the ischemic patients, asynchrony can be expected in any (short-axis) direction. One might speculate that the dispersion in propagation directions for the ischemic patients is related to variable patterns of scar tissue, which influence the propagation.

van de Veire et al. (21), using the time to peak systolic motion, also found a more consistent pattern of asynchrony in nonischemic patients than in ischemic patients, with mainly the lateral wall as the most delayed region; however, they found two nonischemic patients (12%) in whom the septum was the most delayed region, whereas in our study, the lateral wall was always later than the septum. This might be attributed to the difference in the parameter that was studied (motion vs. circumferential strain). Ghio et al. (4), using regional onset time of velocity, found a heterogeneous

pattern of most delayed regions. This might be partly explained by the fact that they didn't separate the ischemic patients from the nonischemic patients in the analysis but might also be related to the use of velocity instead of strain (8). Besides, for studying the direction of propagation, the parameter "most delayed region" is probably more sensitive to noise and outliers in the data than the delay vector, which was used in the present study.

Ischemic versus nonischemic. The fact that the ischemic patients showed less mechanical asynchrony than nonischemic patients, despite similar global function, suggests that mechanical asynchrony contributes less to the impaired ventricular function in ischemic patients than in nonischemic patients. Hence, resynchronization might be less effective in these patients compared with the nonischemic patients, as is also observed in some studies (14,15,22).

The observation that the ischemic patients have a significantly weaker correlation between T_{onset} and $T_{\text{peak,first}}$ might help to explain why it is more difficult to predict the response to CRT for these patients when peak times are used (23). With CRT, one tries to synchronize T_{onset}, whereas the asynchrony measure used to predict the response is based on peak times, which are often not correlated to T_{onset} in individual ischemic patients (Fig. 4).

Study limitations. A limitation of this study is that early shortening before the ECG R-wave is not detected, because the MRI acquisition triggers on the peak R-wave of the ECG. Consequently, T_{onset} times in the septum might be too late. The observed asynchrony in T_{onset} must, therefore, be regarded as a lower bound of the actual asynchrony.

We did not compare the timing of circumferential strain with that of regional velocity, wall motion, or longitudinal strain rates, as can be obtained with echocardiography. Therefore, although this study shows that onset time and (first) peak time of regional function are, in principle, correlated, no firm conclusion can be drawn from this work for the (clinical) use of peak times obtained with echocardiography. Which echocardiographic measure is most suitable for the prediction of the response to CRT, however, seems to be controversial and certainly needs further research (8,23).

Conclusions. Time to first peak ($T_{\text{peak,first}}$) of circumferential shortening and time to maximum peak ($T_{\text{peak,max}}$) both correlated with the onset time of shortening (T_{onset}). $T_{\text{peak,first}}$ performed considerably better than $T_{\text{peak,max}}$, however, and the relations between $T_{\text{peak,first}}$ and T_{onset} in individual subjects were more consistent in the nonischemic patient group than in the ischemic patient group.

For all patients, the longitudinal components of the propagation delay in both T_{onset} and $T_{\text{peak,first}}$ were negligible in comparison with the short-axis component. For the nonischemic patients, the main direction of the propagation of T_{onset} and $T_{\text{peak,first}}$ was consistently from septum to lateral wall. In the ischemic patients, however, no consistent direction was found.

Reprint requests and correspondence: Jaco J. M. Zwanenburg, Department of Physics and Medical Technology, VU University Medical Center, PO Box 7057, 1007 MB Amsterdam, the Netherlands. E-mail: jjm.zwanenburg@vumc.nl.

REFERENCES

1. Nelson GS, Curry CW, Wyman BT, et al. Predictors of systolic augmentation from left ventricular pre-excitation in patients with dilated cardiomyopathy and intraventricular conduction delay. Circulation 2000;101:2703–9.
2. Kass DA. Predicting cardiac resynchronization response by QRS duration: the long and short of it. J Am Coll Cardiol 2003;42:2125–7.
3. Bader H, Garrigue S, Lafitte S, et al. Intra-left ventricular electromechanical asynchrony. A new independent predictor of severe cardiac events in heart failure patients. J Am Coll Cardiol 2004;43:248–56.
4. Ghio S, Constantin C, Klersy C, et al. Interventricular and intraventricular dyssynchrony are common in heart failure patients, regardless of QRS duration. Eur Heart J 2004;25:571–8.
5. Pitzalis MV, Iacoviello M, Romito R, et al. Cardiac resynchronization therapy tailored by echocardiographic evaluation of ventricular asynchrony. J Am Coll Cardiol 2002;40:1615–22.
6. Yu CM, Chau E, Sanderson JE, et al. Tissue Doppler echocardiographic evidence of reverse remodeling and improved synchronicity by simultaneously delaying regional contraction after biventricular pacing therapy in heart failure. Circulation 2002;105:438–45.
7. Bax JJ, Ansalone G, Breithardt OA, et al. Echocardiographic evaluation of cardiac resynchronization therapy: ready for routine clinical use? A critical appraisal. J Am Coll Cardiol 2004;44:1–9.
8. Breithardt OA, Stellbrink C, Herbots L, et al. Cardiac resynchronization therapy can reverse abnormal myocardial strain distribution in patients with heart failure and left bundle branch block. J Am Coll Cardiol 2003;42:486–94.
9. Turner MS, Bleasdale RA, Vinereanu D, et al. Electrical and mechanical components of dyssynchrony in heart failure patients with normal QRS duration and left bundle-branch block: impact of left and biventricular pacing. Circulation 2004;109:2544–9.
10. Penicka M, Bartunek J, De Bruyne B, et al. Improvement of left ventricular function after cardiac resynchronization therapy is predicted by tissue Doppler imaging echocardiography. Circulation 2004;109:978–83.
11. Helm RH, Leclercq C, Faris OP, et al. Cardiac dyssynchrony analysis using circumferential versus longitudinal strain: implications for assessing cardiac resynchronization. Circulation 2005;111:2760–7.
12. Wyman BT, Hunter WC, Prinzen FW, McVeigh ER. Mapping propagation of mechanical activation in the paced heart with MRI tagging. Am J Physiol 1999;276:H881–91.
13. Zwanenburg JJM, Götte MJW, Kuijer JPA, Heethaar RM, Van Rossum AC, Marcus JT. Timing of cardiac contraction in humans mapped by high-temporal-resolution MRI tagging: early onset and late peak of shortening in the lateral wall. Am J Physiol Heart Circ Physiol 2004;286:H1872–80.
14. John Sutton MG, Plappert T, Abraham WT, et al. Effect of cardiac resynchronization therapy on left ventricular size and function in chronic heart failure. Circulation 2003;107:1985–90.
15. Reuter S, Garrigue S, Barold SS, et al. Comparison of characteristics in responders versus nonresponders with biventricular pacing for drug-resistant congestive heart failure. Am J Cardiol 2002;89:346–50.
16. Götte MJW, Zwanenburg JJM, Tecelão SRR, Marcus JT. Propagation of time to onset of shortening in patients with nonischemic dilated cardiomyopathy. In: Proceedings of the 13th Scientific Meeting of the International Society for Magnetic Resonance in Medicine. Miami Beach, FL: ISMRM, 2005:1691.
17. Goldstein H, Rashash J, Plewis I, et al. A User's Guide to MlwiN. Multilevel Models Project, Institute of Education, University of London, 1998.
18. Prinzen FW, Hunter WC, Wyman BT, McVeigh ER. Mapping of regional myocardial strain and work during ventricular pacing: experimental study using magnetic resonance imaging tagging. J Am Coll Cardiol 1999;33:1735–42.
19. Grines CL, Bashore TM, Boudoulas H, Olson S, Shafer P, Wooley CF. Functional abnormalities in isolated left bundle branch block. The effect of interventricular asynchrony. Circulation 1989;79:845–53.
20. Vernooy K, Verbeek XA, Peschar M, et al. Left bundle branch block induces ventricular remodeling and functional septal hypoperfusion. Eur Heart J 2005;26:91–8.
21. van de Veire N, De Sutter J, van Camp G, et al. Global and regional parameters of dyssynchrony in ischemic and nonischemic cardiomyopathy. Am J Cardiol 2005;95:421–3.
22. Lindner O, Vogt J, Kammeier A, et al. Effect of cardiac resynchronization therapy on global and regional oxygen consumption and myocardial blood flow in patients with non-ischaemic and ischaemic cardiomyopathy. Eur Heart J 2005;26:70–6.
23. Yu CM, Fung JW, Zhang Q, et al. Tissue Doppler imaging is superior to strain rate imaging and postsystolic shortening on the prediction of reverse remodeling in both ischemic and nonischemic heart failure after cardiac resynchronization therapy. Circulation 2004;110:66–73.